International Journal of Advances in Electrical Engineering

E-ISSN: 2708-4582
P-ISSN: 2708-4574
Impact Factor (RJIF): 5.6
IJAEE 2026; 7(1): 01-07

www.electricaltechjournal.com
Received: 02-10-2025
Accepted: 05-11-2025

Saif Talal Bahar
Department of Electromechanical Techniques, Baquba Technical College, Middle Technical University, Baghdad, Iraq

Hao Qiu
School of Mechanical and Electrical Engineering, Guilin University of Electronic Technology, Guilin, China

Correspondence
Saif Talal Bahar
Department of Electromechanical Techniques, Baquba Technical College, Middle Technical University, Baghdad, Iraq

Direct torque control constructed on FCS-MPTC of five-phase PMSM drive

Saif Talal Bahar and Hao Qiu

DOI: https://www.doi.org/10.22271/27084574.2026.v7.i1a.110

Abstract
The compact size, strong failure tolerance, low voltage, and great power output of the five-phase permanent magnet synchronous motor (FP-PMSM) are only a few of its benefits. However, its distinct x-y subspace produces greater current harmonics than the three-phase permanent magnet synchronous motor (TP-PMSM). As a result, five-phase systems cannot benefit from direct torque control (DTC). This study examines the DTC basic idea used for a five-phase motor using a traditional model prediction technique and suggests an enhanced model prediction methodology in order to reduce the current harmonics created in the x-y subspace. By streamlining the voltage vector and improving the target function, this technique lowers torque ripple and current harmonics. Simulation findings were used to confirm the theoretical analysis.

Keywords: PMSM, direct torque control, Voltage Vector, FCS-MPTC

1. Introduction
In contrast to the widely utilized TP-PMSM, FP-PMSM has distinctive features such as strong fault tolerance and excellent low-voltage power density in addition to the high efficiency and dependability of PMSMs. When the current per stage is constant, the system's overall power increases due to its various stages [1-2]. As a result, its qualities have been successfully applied in settings that call for little maintenance, challenging working circumstances, and low-voltage, high-power uses. In the marine, submarine, aerospace, and various other industries, for instance, it has become quite popular. In contrast to the widely utilized TP-PMSM, FP-PMSM has distinctive features such as strong fault tolerance and excellent low-voltage power density, in addition to the high efficiency and dependability of PMSMs [3]. When the current per stage is constant, the system's total power increases due to the cumulative effect of its various stages. As a result, its qualities have been successfully applied in settings that call for little maintenance, challenging working circumstances, and low-voltage, high-power uses. In the marine, submarine, aerospace, and other industries, for instance, it has become widely used. Three-phase systems have made extensive use of the DTC technique. DTC relies less on motor parameters and doesn't need complicated coordinate transformations, in contrast to vector control, which is also widely employed [4]. However, there are significant torque swings since the traditional DTC approach only chooses one voltage vector per control cycle. The existence of an x-y subspace causes harmonic currents to arise because the FP-PMSM architecture is different from the TP-PMSM architecture. Consequently, a five-phase motor cannot be immediately equipped with the three-phase DTC algorithm. A steady switching frequency has been attained by studies [5] utilizing the FP-PMSM motor framework, which employs a two-level power inverter for drive and regulation.

2. Materials and Methods
2.1 Mathematical Model of Five-Phase Motor
A five-phase PMSM with a non-sinusoidal back electromotive force needs to be controlled simultaneously in the fundamental plane and the third harmonic plane. As shown in Figure 1, the coordinate system from phase A to phase E is mapped to the fundamental and third harmonic coordinate systems. α1-β1 and α3-β3 are the stationary coordinate systems of the fundamental and third harmonic phases, respectively; d1-q1 and d3-q3 are the rotating coordinate systems of the fundamental and third harmonic phases, respectively; θ_{r1},θ_{r3} represents the electrical angle by which the d-axis leads the α-axis in the fundamental and third harmonic coordinate systems, respectively, where θr3 = 3θr1, θr1 = θr, and θr is the rotor position angle.

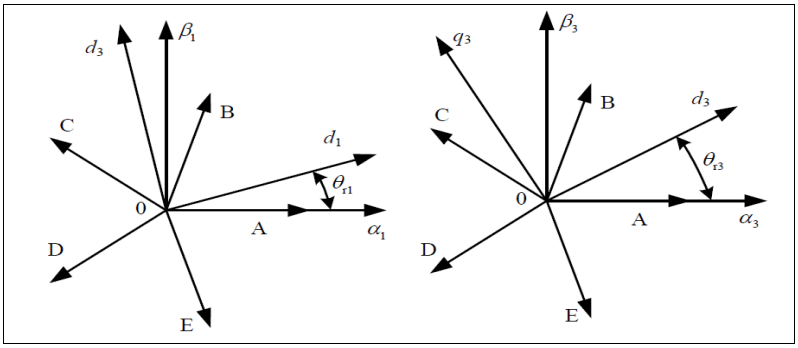

Fig 1: Coordinate system definition

When the motor is stationary, the voltage equations in the two-phase stationary coordinate system are as follows [6]:

$$\begin{bmatrix} u_{\alpha 1} \\ u_{\beta 1} \end{bmatrix} = R \begin{bmatrix} i_{\alpha 1} \\ i_{\beta 1} \end{bmatrix} + \begin{bmatrix} L_{11} + L_{21}\cos 2\theta_r & L_{21}\sin 2\theta_r \\ L_{21}\sin 2\theta_r & L_{11} - L_{21}\cos 2\theta_r \end{bmatrix} \frac{\mathrm{d}}{\mathrm{d}t} \begin{bmatrix} i_{\alpha 1} \\ i_{\beta 1} \end{bmatrix}$$

$$\begin{bmatrix} u_{\alpha 3} \\ u_{\beta 3} \end{bmatrix} = R \begin{bmatrix} i_{\alpha 3} \\ i_{\beta 3} \end{bmatrix} + \begin{bmatrix} L_{13} + L_{23}\cos 6\theta_r & L_{23}\sin 6\theta_r \\ L_{23}\sin 6\theta_r & L_{13} - L_{23}\cos 6\theta_r \end{bmatrix} \frac{\mathrm{d}}{\mathrm{d}t} \begin{bmatrix} i_{\alpha 3} \\ i_{\beta 3} \end{bmatrix}$$

In the formula: L11=(Ld1+Lq1)/2; L21=(Ld1-Lq1)/2; L13=(Ld3+Lq3)/2; L23=(Ld3-Lq3)/2; uα1 and uβ1 are the voltages of the α1 and β1 axes, respectively; uα3 and uβ3 are the voltages of the α3 and β3 axes, respectively; α_{i1} and β_{i1} are the currents of the α1 and β1 axes, respectively; α_{i3} and β_{i3} are the currents of the α3 and β3 axes, respectively; Ld1 and Lq1 are the inductances of the d1 and q1 axes, respectively; Ld3 and Lq3 are the inductances of the d3 and q3 axes, respectively; R is the stator resistance.

2.2 Inverter Output Voltage Vector

The figure 2 switch states are Sa, Sb, Sc, Sd, and Se, where Sn=1 indicates that the upper arm switch (n=a, b, c, d, e) is on and S=0 shows that the bottom arm switch is on [2]. A spatial potential vector consisting of two zero vectors and thirty effective potential vectors corresponds to two total switch states, which constitute 32 switch combinations [7].

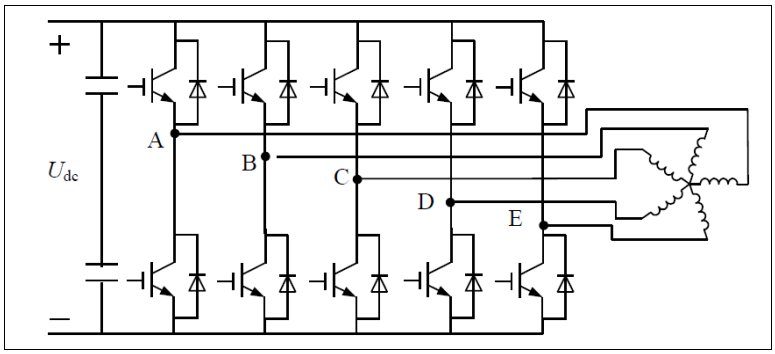

Fig 2: Topology of a five-phase inverter

The distribution of 32 different kinds of area potential vectors in the static location system of the α-β subspace and subspace [8] is depicted in Figure 3.

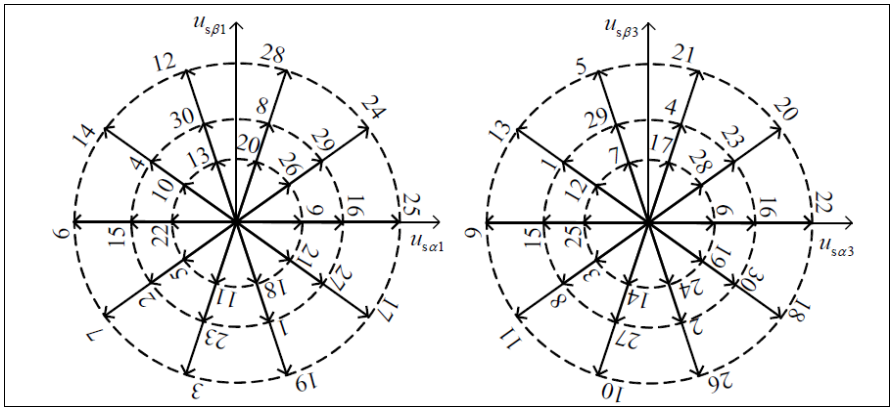

Fig 3: vector diagram of the fundamental voltage

Direct Torque Control Algorithm for Five-Phase Drive Systems

Traditional three-phase DTC algorithms select a suitable voltage vector from a pre-set offline switching table each control cycle based on the control quantity information output by the torque and flux linkage hysteresis comparators. This makes the motor flux linkage trajectory approximate a standard circle, thus continuously and rapidly changing the magnitude of the motor output torque [4]. This principle can also be extended to multi-phase motors. To avoid complex coordinate system rotation transformations, the DTC algorithm is mainly performed in a two-phase stationary coordinate system. The decoupled mathematical model of a five-phase PMSM in the α-β and z1-z2 coordinate systems, including voltage, flux linkage, and torque equations, is summarized in equations (1,2 and 3):

$$\begin{aligned}\psi_\alpha &= L_s i_\alpha + \psi_f \cos\theta_r \\ \psi_\beta &= L_s i_\beta + \psi_f \sin\theta_r\end{aligned} \tag{1}$$

$$\psi_s = \sqrt{\psi_\alpha^2 + \psi_\beta^2} \tag{2}$$

$$T_e = \frac{5P\psi_s\psi_f \sin\delta}{2L_s} \tag{3}$$

The FCS-MPTC system for a five-phase PMSM

The FCS-MPC algorithm is essentially a rolling time-domain optimization algorithm that re-optimizes the objective function at each sampling time. The FCS-MPC algorithm includes two types: FCS-MPCC and FCS-MPTC. This paper explains the working principles of both algorithms, derives the prediction models for applying them to a five-phase PMSM system, designs an objective function suitable for a five-phase PMSM, and finally designs an optimization scheme to address the system delay problem [9]. Implementing FCS-MPCC in a five-phase PMSM system is the foundation for implementing FCS-MPTC. The FCS-MPCC algorithm is relatively simple and easy to implement, only predicting the current, but its control philosophy is consistent with that of the FCS-MPCC algorithm. FCS-MPTC requires simultaneous prediction of torque and flux linkage. First, the stator voltage equation of the five-phase PMSM in dual rotating coordinates, as expressed in Equation 4, is expressed in stator current form:

$$\begin{cases} \frac{d}{dt} i_{d1} = -\frac{R}{L_s} i_{d1} + \frac{L_d}{L_q} \omega_{ei^2 1} + \frac{1}{L_d} u_{d1} \\ \frac{d}{dt} i_{q1} = -\frac{R}{L_q} i_{q1} - \frac{1}{L_q} \omega_e (L_d i_{d1} + \varphi_f) + \frac{1}{L_q} u_{q1} \\ \frac{d}{dt} i_{d3} = -\frac{R}{L_\perp} i_{d3} + \frac{1}{L_d} u_{d3} \\ \frac{d}{dt} i_{q3} = -\frac{R}{L_\perp} i_{q3} + \frac{1}{L_q} u_{d2} \end{cases} \tag{4}$$

Equation 5 is discretized using the forward Euler approximation method, resulting in the discrete state equations shown in Equation 5:

$$\begin{cases} i_{d1}(k+1) = \left(1 - T_s \frac{R}{L_d} i_{d1}\right) i_{d1}(k) + \left(T_s \frac{L_q}{L_d} \omega_e(k)\right) i_{q1}(k) + \frac{T_s}{L_d} u_{d1}(k) \\ i_{q1}(k+1) = \left(1 - T_s \frac{R}{L_q} i_{d1}\right) i_{q1}(k) + \left(T_s \frac{L_d}{L_q} \omega_e(k)\right) i_{d1}(k) + \frac{T_s}{L_q} u_{q1}(k) - \left(\frac{T_s}{L_q} \omega_e(k)\right) \psi_f \\ i_{d3}(k+1) = \left(1 - T_s \frac{R}{L_\perp}\right) i_{d3}(k) + \frac{T_s}{L_d} u_{d3}(k) \\ i_{q3}(k+1) = \left(1 - T_s \frac{R}{L_\perp}\right) i_{q3}(k) + \frac{T_s}{L_q} u_{q3}(k) \end{cases} \tag{5}$$

Where K represents the current sampling time, Ts is the system sampling period. $i_{d1}(k)$、$i_{q1}(k)$、$i_{d3}(k)$、$i_{q3}(k)$ Represent the stat current and voltage at the current sampling time, respectively; $u_{d1}(k)$、$u_{q1}(k)$、$u_{d3}(k)$ and $u_{q3}(k)$. $i_{d1}(k+1)$、$i_{q1}(k+1)$、and $i_{q3}(k+1)$Represent the predicted value of the stator current at the next sampling time; $\omega_e(k)$ Is the electric angular velocity at the current sampling time?

FCS-MPTC first predicts the torque and flux linkage at the current sampling moment using the basic space voltage vector. Then, it selects the optimal voltage vector to apply to the inverter based on the objective function minimization principle [10]. The five-phase PMSM equations are discretized, and the discrete state equations of the motor are obtained using the forward Euler approximation method, as shown in Equation 6:

$$\begin{cases} I_{dq}{}^{k+1} = AI_{dq}{}^{k} + BU_{dq}{}^{k} + C \\ \psi_{dq}{}^{k+1} = L_{dq}I_{dq}{}^{k+1} + \psi_f \\ T_e{}^{k+1} = 5/2N_p\left(\psi_{dq}{}^{k+1} \cdot I_{dq}{}^{k+1}\right) \end{cases} \quad (6)$$

Where $\boldsymbol{I}_{dq}^{k}$ and $\boldsymbol{U}_{dq}^{k}$ Represent the sampled current and voltage vectors of the current control cycle, respectively. $\boldsymbol{I}_{dqq}^{k+1}$、$\boldsymbol{I}_{dq}^{k+1}$ and $\boldsymbol{\psi}_{dqq}^{k+1}$ Represent the predicted values of the sampled current, voltage vector, and flux linkage vector in the next control cycle, respectively, and they are described in a dual rotating coordinate system as follows:

$$\begin{cases} \boldsymbol{I}_{dq}{}^{k} = \left[i_{d11}^{k} \quad i_{q1}^{k} \quad i_{d3}^{k} \quad i_{q3}^{k} \quad i_{0}^{k}\right]^{T} \\ \boldsymbol{U}_{dqk}{}^{k} = \left[u_{d1}^{k} \quad u_{q1}^{k} \quad u_{d3}^{k} \quad u_{q3}^{k} \quad u_{0}^{k}\right]^{T} \\ \boldsymbol{\psi}_{dqq}{}^{k} = \left[\psi_{d1}^{k} \quad \psi_{q1}^{k} \quad \psi_{d3}^{k} \quad \psi_{q3}^{k} \quad \psi_{0}^{k}\right]^{T} \end{cases} \quad (7)$$

Where A, B, and C are coefficient matrices, defined for ease of representation:

$$\begin{cases} \lambda = T_s/L_d \\ \delta = T_s/L_q \\ \eta = T_s/L_{ls} \end{cases}$$

Then A, B, and C can be represented as:

$$\boldsymbol{A} = \begin{bmatrix} 1-\lambda R_s & \lambda L_q \omega_e & 0 & 0 & 0 \\ -\delta L_d \omega_e & 1-\delta R_s & 0 & 0 & 0 \\ 0 & 0 & 1-\eta R_s & 0 & 0 \\ 0 & 0 & 0 & 1-\eta R_s & 0 \\ 0 & 0 & 0 & 0 & 1-\eta R_s \end{bmatrix}$$
$$\boldsymbol{B} = \mathrm{diag}[\lambda \quad \delta \quad \eta \quad \eta \quad \eta]$$
$$\boldsymbol{C} = \mathrm{diag}\psi_f[0 \quad -\omega_e \quad 0 \quad 0 \quad 0] \quad (8)$$

In summary, the designed FCS-MPTC control structure of the five-phase PMSM system driven by the PI controller based on a five-phase two-level inverter can be obtained, as shown in Figure 4.

$$\min\{f_i\} = \left|T_e^* - T_e^{k+1}\right| + k_1\left|\psi_{d1-q1}^* - \psi_{d1-q1}^{k+1}\right| + k_2\left|\psi_{d3-q3}^* - \psi_{d3-q3}^{k+1}\right|$$

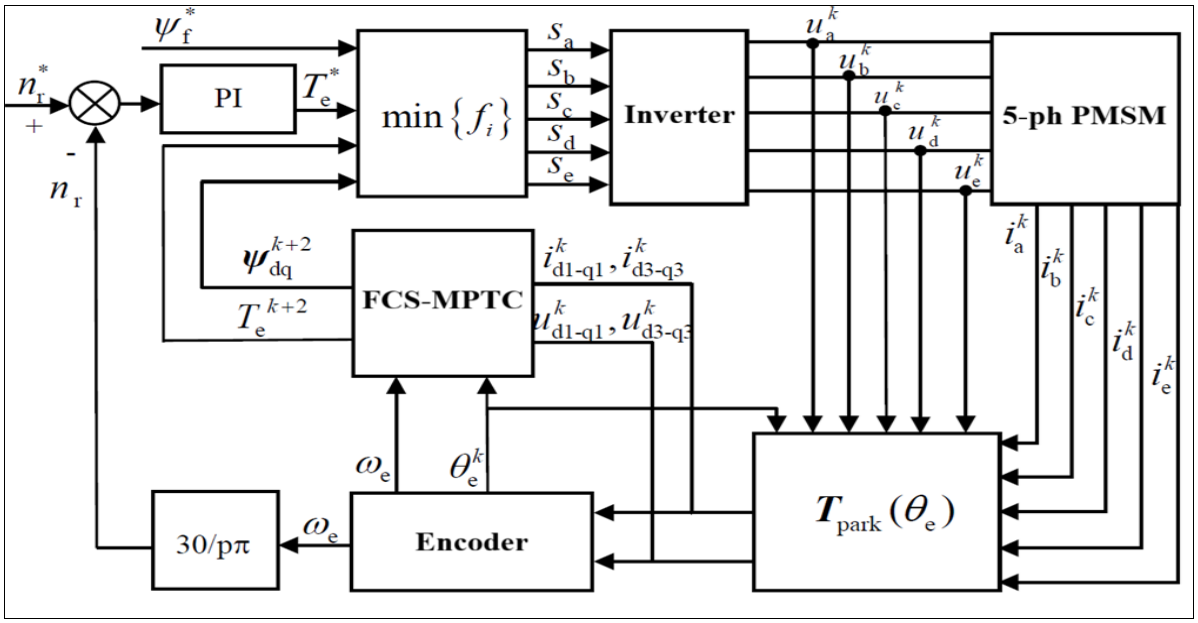

Fig 4: FCS-MPTC control block diagram of a five-phase PMSM

Results and Discussion

To verify the performance of the designed five-phase PMSM FCS-MPTC control system, the corresponding module program was written using S-function programming. The control system depicted in Figure 4 was developed using the MATLAB/Simulink simulation platform, and subsequent simulation experiments were conducted. Simultaneously, the simulation results were compared with the DTC algorithm of the five-phase PMSM system .The electromagnetic torque setpoints in both the FCS-MPTC and DTC systems are obtained by PI controllers. The relevant parameters of the five-phase PMSM during the simulation are shown in Table 1.

Table 1: Lists simulation parameters of the five-phase PMSM used for performance evaluation.

Parameter	Value	Unit
load torque	12	N.m
Dc-link voltage	300	V
P	3	-
Rs	0.5	Ω
Ld=Lq	12.4	mH
J	0.02	$kg.m^2$
PM flux	0.09	Wb

As evidenced by the graphical representations provided in Figures 5 and 6, it is abundantly clear that the actual speed response of the system closely adheres to the predetermined reference speed across a spectrum of varying set values, which include 300, 400, 600, 700, and 800 revolutions per minute (rpm). Specifically, Figures 5 and 6 serve to depict, in detail, the dynamic speed response characteristics of the two distinct control systems when subjected to a sudden load disturbance, thereby offering a comparative analysis of their respective performances under such conditions. To facilitate a rigorous and unbiased comparative evaluation, it was imperative to meticulously adjust the parameters of the (PI) controller, which consequently enabled the manipulation of the speed response curves of the (FCS-MPTC) structure, thereby achieving a state of equilibrium in the steady-state errors before the application of the load. This strategic approach aimed to ensure that the initial steady-state value was effectively harmonized, thus allowing for an accurate representation of the control systems' capabilities in maintaining desired operational stability.

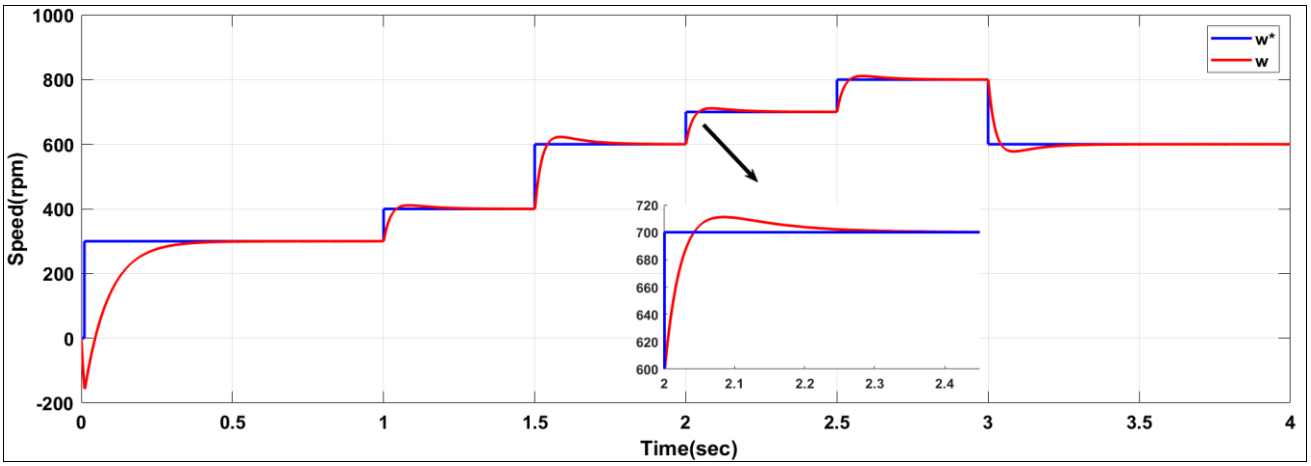

Fig 5: Speed curve of DTC control system

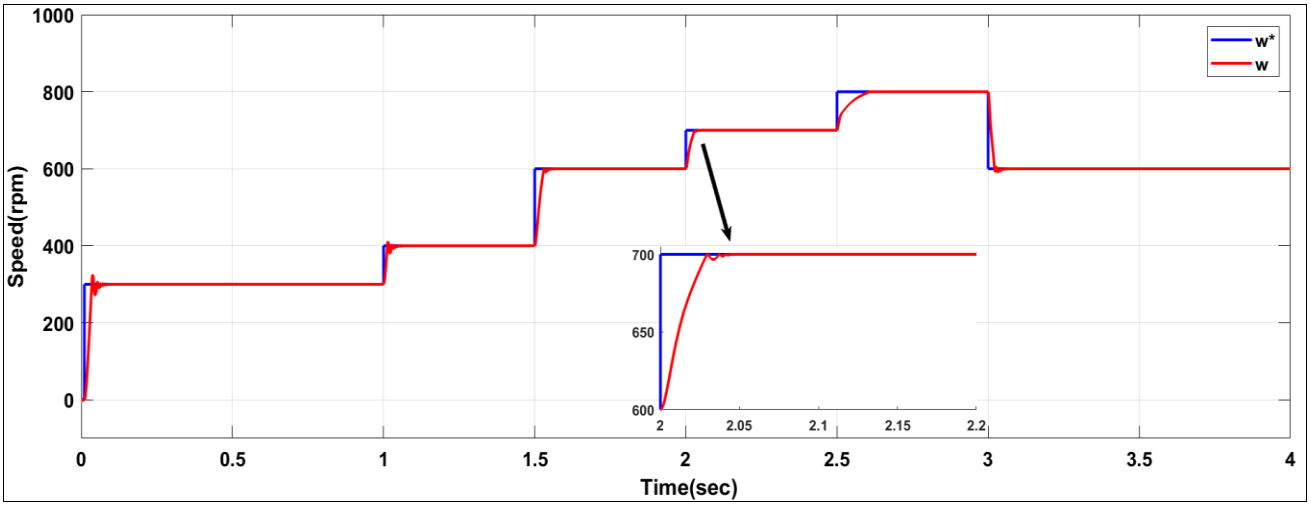

Fig 6: Speed response curve of the speed control system based on FCS-MPTC.

Figure 7 illustrates the discrepancies in speed measurement that are characteristic of Direct Torque Control (DTC) methodology. The magnitude of the overshoot associated with the error is notably substantial, suggesting a significant deviation from the desired performance metrics. Specifically, at the temporal marker of 1.5 seconds, one can observe that the error exhibits an overshoot that peaks at a value of 200, indicating a considerable departure from the intended operational parameters; conversely, at the 3-second mark, this phenomenon is reversed, with the error demonstrating an overshoot that plummets to -200. This oscillatory behavior in the error signals has pertinent implications for the control strategy employed, necessitating a comprehensive analysis to mitigate such pronounced deviations in future implementations. Figure 8 shows the speed error in FCS-MPTC. The overshoot of the error is great. At 1.5 s, the error is seen to be overshoot 21, and at 3 s, the overshoot is -21. The results showed the effect of using (FCS-MPTC) on the speed error reduction.

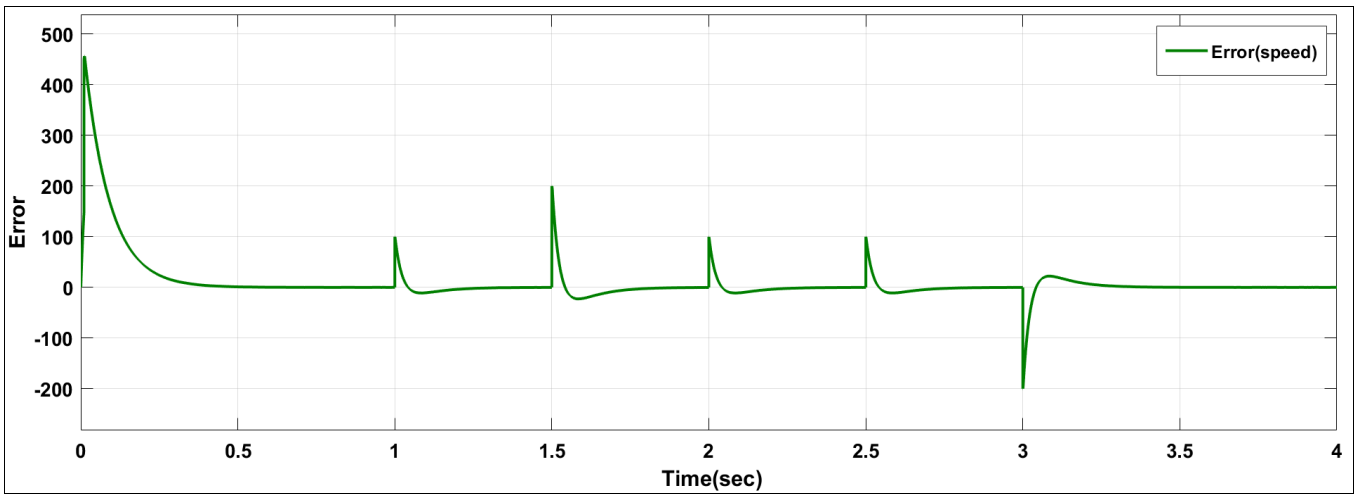

Fig 7: Error with DTC

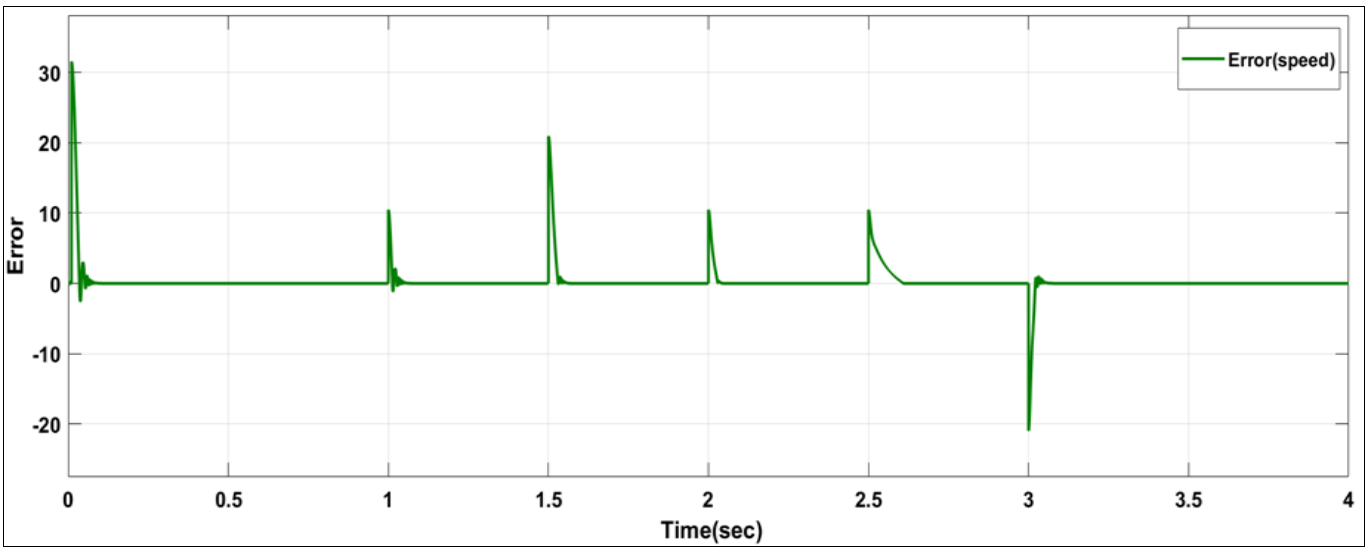

Fig 8: Error with FCS-MPTC

Conclusion

A multi-phase permanent magnet synchronous motor (PMSM)has the advantages of great power density, more control freedom, and good fault-tolerant performance compared with the traditional three-phase motor control system. At present, direct torque control (DTC) is the most widely used in the control field of multi-phase PMSM. However, the DTC algorithm has the disadvantages of large torque ripple and low equivalent switching frequency. Finite control set model predictive torque control (FCS-MPTC) can directly consider the constraints of the input and output of the controlled process to handle multivariable, highly coupled systems. It can significantly improve the shortcomings of the above DTC, and it has the characteristics of fast dynamic response and flexible control.

References

1. Okazaki K, Yang K, Akatsu K. Real-time dynamic eccentricity detection by analyzing harmonic components of no-load line-line voltages in multi-three-phase PMSMs. IEEJ Journal of Industry Applications. 2023;12(3):409-417.
2. Bahar ST, Omar RG. Torque ripple alleviation of a five-phase permanent magnet synchronous motor using predictive torque control method. International Journal of Power Electronics and Drive Systems. 2022 Dec;13(4):2207-2215. doi:10.11591/ijpeds.v13.i4.pp2207-2215.
3. Niu G, Dong X, Chen Y. Motor fault diagnostics based on current signatures: a review. IEEE Transactions on

Instrumentation and Measurement. 2023;72:1-19.
4. Zheng BL, Fletcher JE, He X. A novel direct torque control scheme for a sensorless five-phase induction motor drive. IEEE Transactions on Industrial Electronics. 2011 Feb;58(2):503-513.
5. Ren Y, Zhu ZQ. Reduction of both harmonic current and torque ripple for dual three-phase permanent-magnet synchronous machine using modified switching-table-based direct torque control. IEEE Transactions on Industrial Electronics. 2015 Nov;62(11):6671-6683.
6. Bahar ST, Neama R. Improved direct torque control utilizing model predictive control approach for permanent magnet synchronous motor. Al-Iraqia Journal of Scientific Engineering Research. 2024 Jul;3(2). doi:10.58564/ijser.3.2.2024.179.
7. Sakthisudhursun B, Pandit JK, Aware MV. Simplified three-level five-phase SVPWM. IEEE Transactions on Power Electronics. 2016 Mar;31(3):2429-2436.
8. Bahar ST, Abd-Alhmeed RA. Reduce-complexity of predictive current control for a 3-phase voltage source inverter. JT. 2025 Sep;7(3):16-25. doi:10.51173/jt.v7i3.2621.
9. Tatte YN, Aware MV. Torque ripple minimization in five-phase three-level inverter-fed direct torque control induction motor drive. In: Proceedings of the 17th European Conference on Power Electronics and Applications; 2015. p. 1-6.
10. Bahar ST, Qiu H, Neama DR, Hashim FF, Yasseen H. An improved cost function based on model predictive current control for five-phase PMSM. Ejeee. 2025 Oct;3(1):32-38. doi:10.62909/ejeee.2025.004.